International Journal of Nanomedicine

Dovepress
open access to scientific and medical research

Open Access Full Text Article

ORIGINAL RESEARCH

Toxicity, biodistribution and oxidative damage caused by zirconia nanoparticles after intravenous injection

This article was published in the following Dove Press journal:
International Journal of Nanomedicine

Yue Yang[1,2]
Huihui Bao[1]
Qianqian Chai[3]
Zhiwen Wang[2]
Zhenning Sun[2]
Changhui Fu[3]
Zhaoping Liu[1]
Zhongjie Liu[2]
Xianwei Meng[3]
Tianlong Liu[2]

[1]China National Center for Food Safety Risk Assessment, Beijing 100022, People's Republic of China; [2]Key Laboratory of Animal Epidemiology of Ministry of Agriculture, College of Veterinary Medicine, China Agricultural University, Beijing 100193, People's Republic of China; [3]Laboratory of Controllable Preparation and Application of Nanomaterials, Technical Institute of Physics and Chemistry, Chinese Academy of Sciences, Beijing 100190, People's Republic of China

Background: As a promising nanomaterial for biomedical applications, zirconia nanoparticles (ZrO_2) have aroused concern recently, but the toxicity of ZrO_2 in vivo has received little attention.

Purpose: The aim of this study is to demonstrate the systematic single dose toxicity, biodistribution and oxidative damage of ZrO_2 in vivo after intravenous injection in mice.

Materials and methods: Ten ICR mice were used at the high dose of ZrO_2 including 600, 500, 400 and 300mg/kg. Maximum tolerated dose (MTD) of 150 nm ZrO_2 was determined as 500mg/kg. Hematology analysis and blood biochemical assay were determined for the evaluation of oxidative damage caused by ZrO_2. Biodistribution of ZrO_2 was investigated by ICP-OES and TEM.

Results: Mice treated with higher dose (500mg/kg) showed significant spread in white blood cell counts ($p<0.05$). Especially, the serum ALT levels of 500mg/kg groups increased significantly ($p<0.05$) compared with the control group. ZrO_2 particles would not induce any changes in appearance and micromorphology of liver at 100 and 350mg/kg. Spleen samples showed no significant changes in micromorphology of the lymphoid follicles and in the size of the red pulp after injection of ZrO_2 at all doses. The serum of ZrO_2-treated animals (350 and 500mg/kg) has reduced levels of SOD compared to the control group ($p<0.05$). ZrO_2 persists in membrane-enclosed vesicles called lysosomes in the liver and spleen macrophages without abnormal changes of ultrastructure.

Conclusion: These findings would contribute to the future development of ZrO_2-based drug delivery system and other biomedical applications.

Keywords: zirconia nanoparticles, toxicity, biodistribution, oxidative damage, ICP-OES

Introduction

As a novel nanomaterial, zirconium oxide (ZrO_2) has made outstanding development in the field of biological applications in recent years.[1–3] ZrO_2 nanoparticles have been applied in dentistry, metal joint, drug carrier and other fields due to their good biocompatibility and strong stability.[4–7] Especially in dentistry, dental materials based on ZrO_2 have been the mainstream of high-end products because of the following advantages of these materials including strong corrosion resistance, pure white color and good compatibility.[8–11] As metal joint, ZrO_2 has significant advantages as good biocompatibility, strong stability and flexural strength.[12] In the latest study, zirconia nanoparticles were successfully used as delivery system to achieve CT imaging and microwave thermal therapy simultaneously. Hollow ZrO_2 nanostructure was used as a carrier to encapsulate ionic liquid (IL), which integrates the CT imaging function of the ZrO_2 shell and the microwave susceptibility function of the IL core.[13]

Correspondence: Huihui Bao
China National Center for Food Safety Risk Assessment, No. 37, Guangqu Road, Chaoyang District, Beijing 100022, People's Republic of China
Tel +105 216 5518
Email baohuihui@cfsa.net.cn

Xianwei Meng
Laboratory of Controllable Preparation and Application of Nanomaterials, Technical Institute of Physics and Chemistry, Chinese Academy of Sciences, No. 29 East Road Zhongguancun, Beijing 100190, People's Republic of China
Tel +108 254 3521
Email mengxw@mail.ipc.ac.cn

Although zirconia nanoparticles displayed great perspective in medical application, the lack of systemic toxicity research of zirconia nanoparticles in vivo and in vitro is key obstacle that holds back further development in medicine. There were some toxicity evaluations of zirconia as dentistry materials; however, few researches focus on toxicity of nanoscale zirconia materials.[14,15] Pilot studies of toxicity researches of zirconia nanomaterials have focused on cell culture systems, nevertheless, the data from these studies could be misleading and will require verification from animal experiments.[16–18] The fate, kinetics, clearance, metabolism, immune response and toxicity of zirconia nanostructures in vivo are urgently needed.

In the manuscript, the acute toxicity of zirconia nanoparticles with hollow structure was examined when they entered the bloodstream by intravenous injection for one time. ZrO_2 was synthesized via a simple, scalable method. These particles have hollow structure, mesopores, controllable size and narrow size distribution. MDA, SOD, CAT and GSH in serum were examined of mice received ZrO_2 in the study and the oxidative stress may play an important role in the ZrO_2 induced toxicity in mice. For better understanding the fate of nanoparticles entered the body, biodistribution in different organs and clearance of ZrO_2 were also investigated.

Materials and methods

Fabrication and characterization of hollow ZrO_2 nanoparticles

Zirconium (IV) propoxide was purchased from Tokyo Chemical Industry Co. Ltd. 1,4-Dioxane and sodium hydroxide (NaOH) were obtained from the Beijing Chemical Reagents Company (China). Aqueous ammonia was a commercially available product. All reagents used in the work were analytical reagents (A.R.) without any further purification. Hollow ZrO_2 nanoparticles were prepared via a template method as previously described.[2,3] Briefly, silica nanoparticles (SN) were employed as templates. SN nanoparticles underwent the dewatering process prior to being dispersed in a mixture of alcohol and acetonitrile. Ammonia was added into adjust the pH value reach to weakly alkaline. The zirconium precursor was slowly injected into the mixture under magnetic stirring. The hydrolytic process of zirconium was triggered in the weakly alkaline environment to induce the growth of small ZrO_2 nanoparticles with SN as seeds. After 6-hr reaction, ZrO_2 shell was formed gradually on the surface of the SN seeds. The thickness of the shell can be controlled by adjusting the reaction time and the ratio of the Zr:SN. To remove the SN seed core, NaOH solution (1 mL, 1 M) was added under a temperature of 80°C for approximately 4 hrs. The obtained hollow ZrO_2 nanoparticles were collected by centrifugation and washed three times with deionized water. Morphology and structure of the resulting ZrO_2 nanoparticles were observed with a JEOL-200CX transmission electron microscope (TEM). The average size and surface charge of the ZrO_2 in 5% glucose were measured by Zetasizer 3000HSA (Malvern) at 25°C. An endotoxin assay showed that there was no detectable gram-negative endotoxin at a concentration of 1 mg/mL (the detection limit was less than 0.1 EU/mL).

Animal experiments

Female ICR mice (provided by Weitonglihua experimental animal Co., Ltd), aged 6–8 weeks, were used in the experiments. Every five mice were housed in stainless steel cages containing sterile paddy husk as bedding in ventilated animal rooms. They were acclimated in the controlled environment (temperature: 22±1°C; humidity: 60±10% and light: 12-hr light/dark cycle) with free access to water and a commercial laboratory complete food. Animal experimentation was governed by the Regulations of Experimental Animals of Beijing Authority. Animal Ethics Committee of the China Agriculture University approved the experiment.

Single dose toxicity

In the dose probing study, 10 ICR mice were used at the high dose of ZrO_2 including 600, 500, 400 and 300 mg/kg (Table S1). For single dose toxicology research of ZrO_2, a series of doses (100, 175, 245, 350 and 500 mg/kg) were set based on pilot study as the described earlier. Intravenous injections of ZrO_2 suspension in sterile 5% glucose were administrated through the mouse tail vein. Intravenous injections of sterile 5% glucose were also given to mice as controls by intravenous. The body weights of mice were measured and recorded through the entire experiments. If mice died in the process, the bodies were sent for an immediate necropsy. At 14 days after injection, all animals were sacrificed and samples were collected.

Coefficients of liver, spleen and kidneys

After weight and sacrifice, the tissues and organs, such as heart, liver, spleen, kidneys, lung and brain were excised and weighed accurately. The coefficients of these tissues, such as

liver, kidneys and spleen to body weight were calculated as the ratio of tissues (wet weight, mg) to body weight (g).

Hematology analysis and blood biochemical assay

At 14 days, blood was drawn for hematology analysis (potassium EDTA collection tube) using a standard saphenous vein blood collection technique. Standard hematology markers were selected for analysis as follows: red blood cell count, hemoglobin, hematocrit, mean corpuscular volume, mean corpuscular hemoglobin, mean corpuscular hemoglobin concentration, platelet count and white blood cell count. Blood samples collected via the ocular vein (about 0.8–1 mL each mouse) were centrifuged twice at 3,000 rpm for 10 mins in order to separate serum. In the present study, liver function was evaluated with serum levels of alanine aminotransferase (ALT), and aspartate aminotransferase (AST). Nephrotoxicity was determined by blood urea nitrogen (BUN) and creatinine (Cr). These parameters were all assayed using a Biochemical Auto analyzer (Type 7170, Hitachi, Japan).

Histopathological examinations

Tissues recovered from the necropsy were fixed in 10% formalin, embedded in paraffin, sectioned, and stained with hematoxylin and eosin (HE) for histological examination using standard techniques. After hematoxylin-eosin staining, the slides were observed and photos were taken using optical microscope (Olympus X71, Japan). All the identity and analysis of the pathology slides were blind to the pathologist.

Biochemical analysis of oxidative stress

Serum was isolated in the form of clear supernatant which was further utilized for determination of endogenous antioxidants status superoxide dismutase (SOD), catalase (CAT), malonaldehyde (MDA) and reduced glutathione (GSH). SOD, CAT, GSH and MDA test kits were purchased from Nanjing Jiancheng Bioengineering Institute (China). The assay for total SOD was based on its ability to inhibit the oxidation of oxymine by the xanthine–xanthine oxidase system.[19] The hydroxylamine nitrite produced by the oxidation of oxymine had an absorbance peak at 550 nm. One unit of SOD activity was defined as the amount that reduced the absorbance at 550 nm by 50%. CAT activity was assayed following the procedure which is based on the rate of decrease of H_2O_2 at 240 nm with detection limit of 0.002 U/mL.[20] Thiobarbituric acid reaction (TBAR) method was used to determine the MDA which can be measured at the wavelength of 532 nm by reacting with thiobarbituric acid (TBA) to form a stable chromophoric production.[21] Analysis of GSH was performed with the method using DTNB as a substrate at 412 nm with detection limit of 1.6 mmol/L.[22]

Stability of ZrO_2 NPs in simulate body fluid

Stability of ZrO_2 NPs in different simulate fluid was investigated including the simulated gastric fluid (SGF, pH=1.2), simulated intestinal fluid (SIF, pH=8.3) and simulated body fluid (pH=7.4). A total of 10 mg ZrO_2 NPs was added into 10 mL different fluids as described earlier, respectively. Then, the suspension was shocked at 20 r/min for 30 days. At 1, 3, 7, 14 and 30 days, samples were collected for particle size measurement by DLS and TEM observation.

TEM imaging of tissues

For electron microscopy, liver and spleen tissues were excised at 24 hrs after ZrO_2 injected at 50 mg/kg and immediately fixed in 3% glutaraldehyde overnight, and then the samples were treated according to the general protocols for TEM study. The ultrathin sections (60 nm) were stained with lead citrate and uranyl acetate. The sections were viewed on a Hitachi H-7650 TEM, operating at 80 kV. All the identity and analysis of the ultrathin section were blind to the pathologist.

Zr content analysis

For in vivo bio-distribution studies, the mice injected at 50 mg/kg dose were sacrificed after injection for 1 day, 1 week and 4 weeks after injection. And brain, heart, kidney, liver, lung and spleen were collected. To determine the Zr content in the tissues, the wet samples were weighed, digested with nitric acid by heating and then analyzed for Zr content using inductively coupled plasma optical emission spectrometer (ICP-OES, NexION 300X).

Statistics

Results were expressed as mean±standard deviation (S.D). Multigroup comparisons of the means were carried out by one-way analysis of variance (ANOVA) test using SPSS 14.0 (SPSS Inc., Chicago, IL). The statistical significance for all tests was set at $p<0.05$.

Results and discussion

Preparation and characterization of ZrO_2

ZrO_2 had well monodispersion in deionized water (Figure 1A) and the wall is about 10 nm by TEM observation. The average

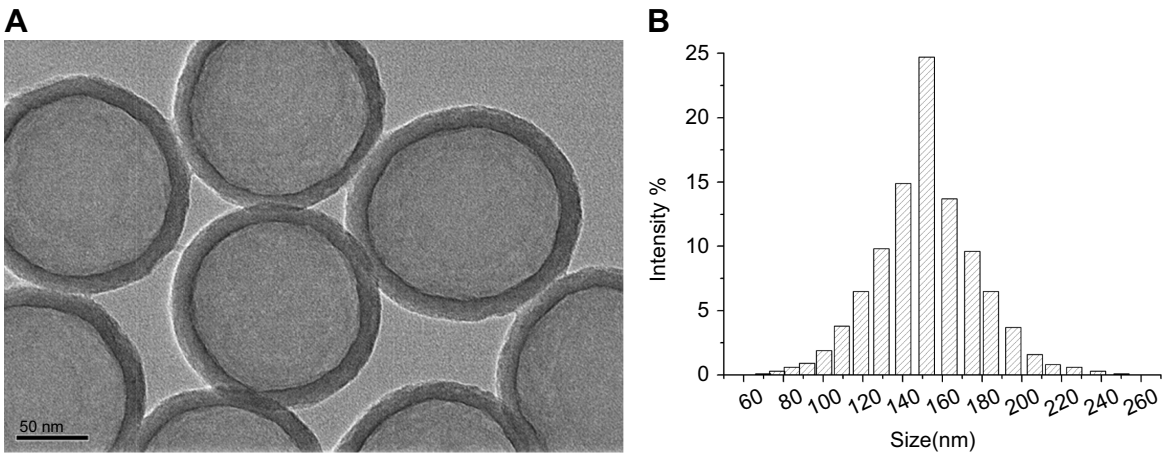

Figure 1 (**A**) The TEM images and (**B**) the average size of ZrO_2 by Zetasizer 3000HSA.

size of the nanoparticles was about 150 nm by Zetasizer 3000HSA (Malvern) at 25°C (Figure 1B). ZrO_2 was sterilized by UV irradiation for 3 hrs, then suspended in sterile 5% glucose and sonicated for 15 mins before being loaded into 1 mL syringes under sterile conditions. The surface characterization of the particles in 5% glucose before and after sonication and irradiation was listed in Table S3. These results indicate that the pre-treatment of sonication and irradiation did not change the physicochemical property of ZrO_2.

Single dose toxicity of ZrO_2

In the dose probing study, no mice injected with ZrO_2 died at 600 mg/kg (Table. S1); however, the body weight of the treated mice decreased over 10% which indicated that the maximum tolerated dose of ZrO_2 was lower than 600 mg/kg. To determine detailed single dose toxicity of ZrO_2, experimental animals were dosed at different levels (100, 175, 245, 350 and 500 mg/kg) according to the preliminary experimental results. After exposure, the mortality in each dose group was observed through the entire experiment. In all the treated groups, no death and unusual behaviors were observed, including vocalizations, labored breathing, difficulties moving, hunching or unusual interactions with cage mates. While the mice received ZrO_2 at 500 mg/kg obviously appeared body weight decreased over 10% after 24 hrs injection than the initial value (Figure S1A). The coefficients of major organs such as liver, spleen, heart, kidney, lung and brain were calculated when they recovered after sacrificed at 14 days. No significant changes were observed in coefficient indexes after administration of ZrO_2 at all doses (Figure S1B).

Hematology and blood biochemical assay

Representative hematology results indicated that measured factors were within normal ranges, and there was no significant difference of all index between groups of low dose (100, 175, 245 and 350 mg/kg) and the control (Figure 2). Mice treated with higher dose (500 mg/kg) showed significant spread in white blood cell counts ($p<0.05$) (Figure 2A). Meanwhile, there was no obvious difference of other indexes in the group received ZrO_2 at 500 mg/kg compared to the control mice. For blood biochemical assay, the ALT levels changed from all treatment groups revealed a dose-dependent manner after intravenous injection. Especially, the serum ALT levels of 500 mg/kg groups increased significantly ($p<0.05$) compared with the control group. (Figure 3-ALT) No significant changes were observed in other biochemical indexes after administration of ZrO_2 at all doses (Figure 3).

Pathological changes in mice

According to the previous research, inorganic nanomaterials mostly caused the damage to the liver. In the present study, similar observation was found. Figure 4 shows ZrO_2 particles would not induce any changes in appearance and micromorphology of liver at 100 and 350 mg/kg. In contrast, lymphocytic infiltration, microgranulation and degenerative necrosis of hepatocytes were obviously observed at 500 mg/kg (Figure 4D). Spleen samples showed no significant changes in micromorphology of the lymphoid follicles and in the size of the red pulp after injection of ZrO_2 at all doses (Figure 5). Kidney and lung samples also showed no remarkable change in the morphology (Figure S2 and S3). No obvious change was observed in the liver, spleen, kidney

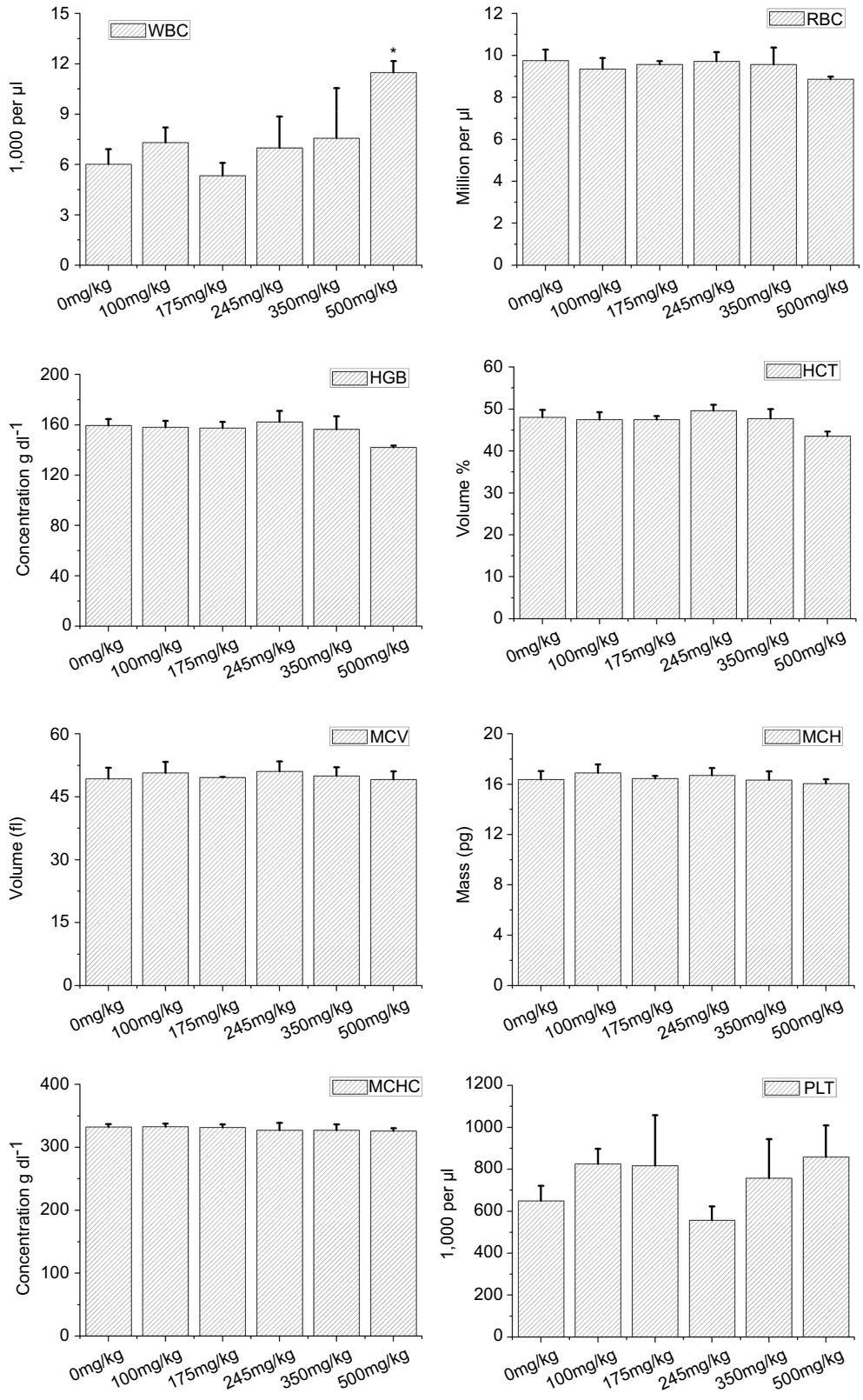

Figure 2 Complete blood counts of ICR mice following injection of ZrO_2. Mean and standard deviation of red blood cell (RBC) numbers, hemoglobin concentration (HGB), hematocrit (HCT), mean corpuscular volume (MCV), mean corpuscular hemoglobin (MCH), mean corpuscular hemoglobin concentration (MCHC), white blood cells (WBC) or platelet (PLT) of ICR mice (n ¼ 10). No statistically significant changes were observed between groups, with the exception of significant spread in WBC counts in 500 dose group of ZrO_2 particles (*denotes statistical significance for the comparison of control, *p<0.05).

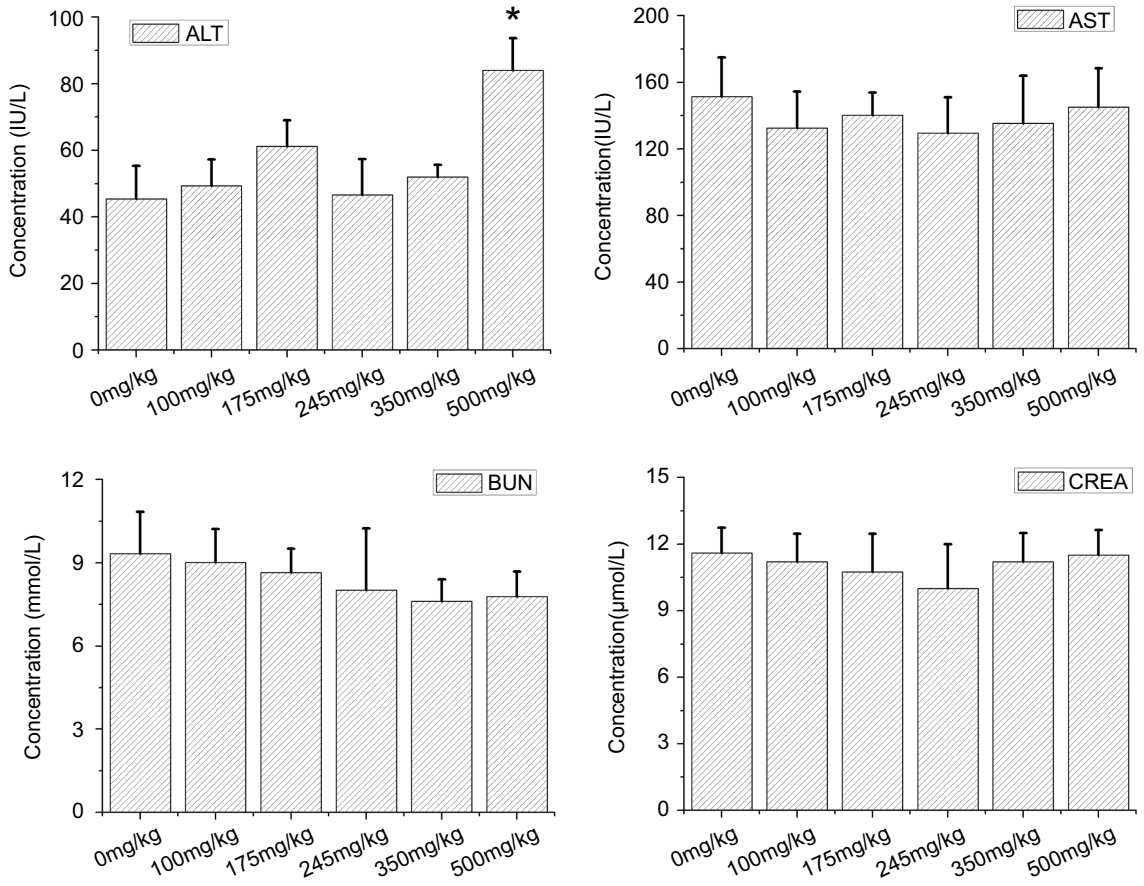

Figure 3 Biochemistry indexes of ICR mice following single injection of ZrO_2. Mean and standard deviation of alanine aminotransferase (ALT), aspartate aminotransferase (AST), blood urea nitrogen (BUN) and creatinine (CREA) of ICR mice (n=10 per group). The serum ALT level of the 500 mg/kg groups increased significantly ($p<0.05$) comparing with control. (*denotes statistical significance for the comparison of control, *$p<0.05$).

and lung samples of 175 and 245 mg/kg group (Figure S4 and S5). These above results indicate low acute toxicity of ZrO_2 when they enter the body by intravenous injection and ZrO_2 mainly caused damage to liver in the experiment. Furthermore, these results revealed a dose-dependent manner of ZrO_2 after single injection.

Indexes of oxidative stress

The antioxidant enzyme superoxide dismutase (SOD) converts superoxide radicals to hydrogen peroxide or oxygen and water. For serum samples, Figure 6A shows that the serum of ZrO_2-treated animals (350 and 500 mg/kg) has reduced levels of SOD compared to the control group ($p<0.05$). Catalase protects cells from oxidative damage by converting hydrogen peroxide to water and oxygen. Figure 6B shows that catalase activity in serum is decreased in mice received ZrO_2 (500 mg/kg) compared to untreated control mice ($p<0.05$). Figure 6C shows the content of MDA in the serum. As is shown in Figure 6C, in the blood serum, the MDA content of ZrO_2 group (500 mg/kg) is much higher than that of control group ($P<0.05$). No significant changes were observed of these above three indexes between the other dose groups compared to the control. Reduced glutathione (GSH) is an antioxidant that protects from damage caused by reactive oxygen species. Figure 6D shows that no obvious difference was observed between the mice received ZrO_2 and the control animals. The results of SOD, CAT, MDA and GSH in the serum of 100 and 175 mg/kg groups were listed in the Table S2. No obvious difference was observed of these four indexes between the mice received ZrO_2 at 100 and 175 mg/kg and the control animals.

For liver sample, Figure 7A shows that the reduced levels of SOD in the liver of ZrO_2-treated animals (500 mg/kg) when compared to the control group. ($p<0.05$) Figure 7B shows that catalase activity in liver is decreased in mice received ZrO_2 (500 mg/kg) compared to untreated control mice ($p<0.05$). As is shown in Figure 7C, in the liver samples, the MDA content of ZrO_2 group (500 mg/kg) is much higher than that of control group ($p<0.05$). No significant changes were observed of these above three indexes between

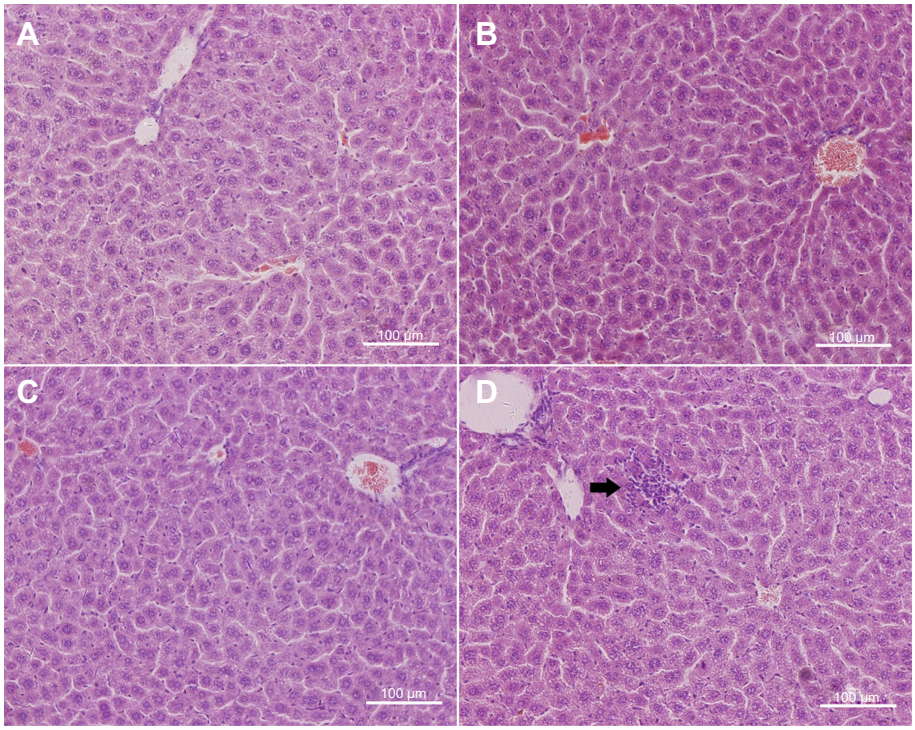

Figure 4 Hematoxylin and eosin-stained images of the liver from control (**A**) and mice injected ZrO_2 at the dose 100 mg/kg (**B**), 350 mg/kg (**C**) and 500 mg/kg (**D**). Black arrow indicates lymphocytic infiltration. (Bar is 100 µm).

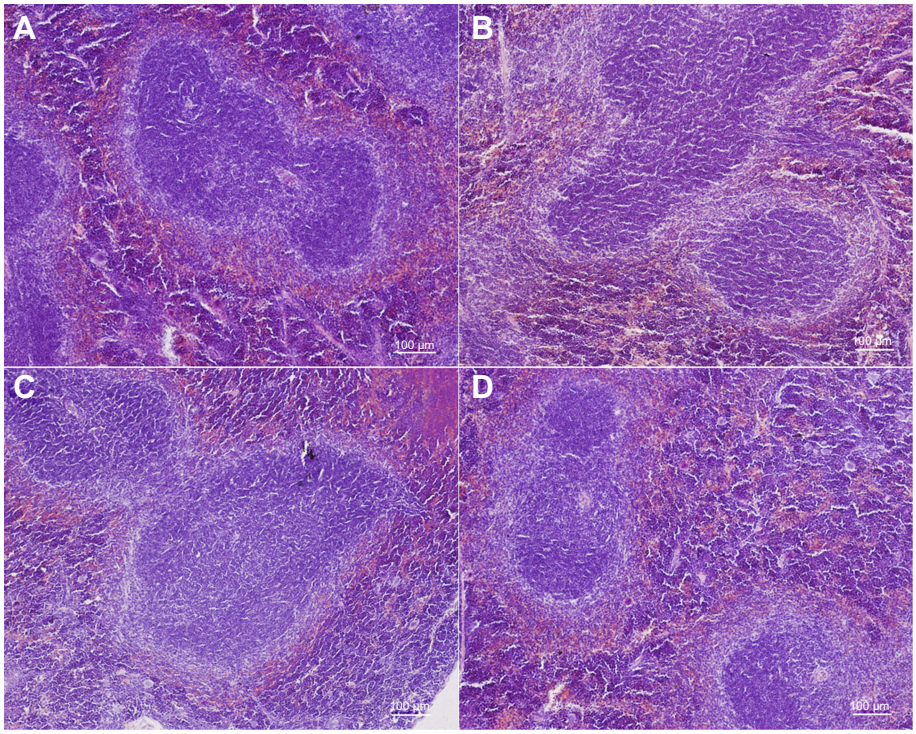

Figure 5 Hematoxylin and eosin-stained images of the kidney from control (**A**) and mice injected ZrO_2 at the dose 100 mg/kg (**B**), 350 mg/kg (**C**) and 500 mg/kg (**D**). (Bar is 100 µm).

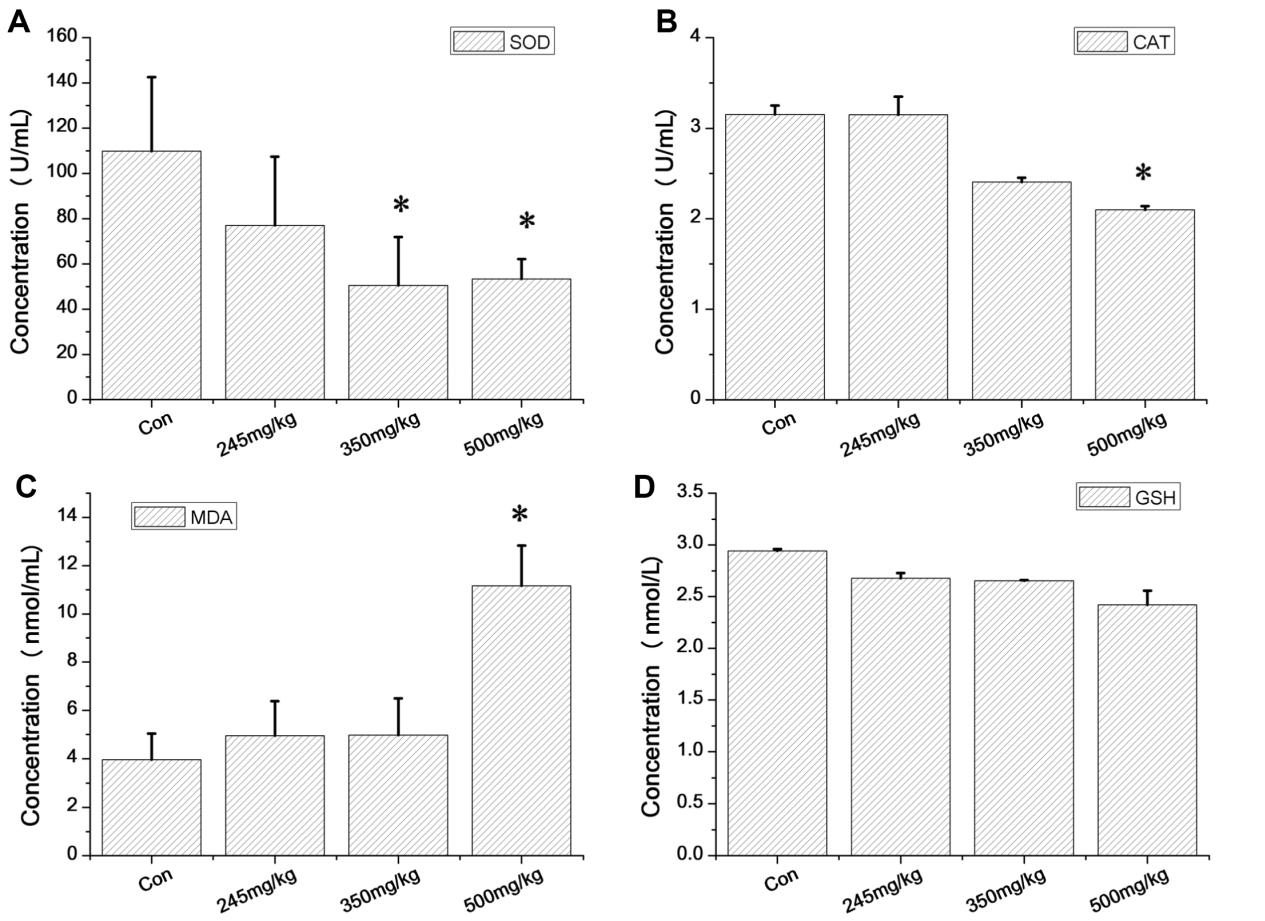

Figure 6 Oxidative stress indexes in the serum of ICR mice following single injection of ZrO_2. Mean and standard deviation of SOD, CAT, MDA and GSH of ICR mice (n=5 per group). The serum SOD level of the 350 and 500 mg/kg groups decreased significantly ($p<0.05$) comparing with control. The CAT level of the 500 mg/kg groups decreased significantly ($p<0.05$) comparing with control. The MDA level of the 500 mg/kg groups increased significantly ($p<0.05$) comparing with control. (*denotes statistical significance for the comparison of control, *$p<0.05$).

the other dose groups compared to the control. Meanwhile, no obvious difference was observed of GSH between the mice received ZrO_2 and the control animals (Figure 7D). The results of SOD, CAT, MDA and GSH in the liver of 100 and 175 mg/kg groups were listed in the Table S2. No obvious difference was observed of these four indexes between the mice received ZrO_2 at 100 and 175 mg/kg and the control animals.

Oxidative stress is a result of imbalance between the antioxidant defense system and the formation of reactive oxygen species (ROS), which has been recognized deleterious due to the damage to cell membranes and DNA. Oxidative damage may cause cell damage, death and exacerbate several chronic diseases including cancer, fatty liver, hepatic fibrosis and Alzheimer's disease. In recent decades, oxidative stress caused by NMs has attracted an increasing attention. Especially, the role of oxidative stress play in the liver damage caused by NMs has aroused concerns. In the present study, the results show that ZrO_2 can cause oxidative stress to the liver. These indicate the liver maybe the major target organs of ZrO_2 when they entered the body by intravenous injection.

Ultrastructure localization of ZrO_2

To investigate the distribution and the fate of particles in vivo, ZrO_2 was injected intravenously at 50 mg/kg in mice. The uptake of nano-structures by macrophage was visualized by TEM observation. ZrO_2 persists in membrane-enclosed vesicles called lysosomes in the liver (Figure 8) and spleen (Figure 9) macrophages without unnormal changes of ultrastructure. In the liver, lots of ZrO_2 were found in the Kupffer cells (KCs) instead of hepatocyte shown in white circle in Figure 8A. The magnified images of the particles (Figure 8B and C) show the original structure of ZrO_2 in the lysosomes. Compared with the liver, less ZrO2 were found in the macrophage of the spleen (Figure 9A and B). The particle

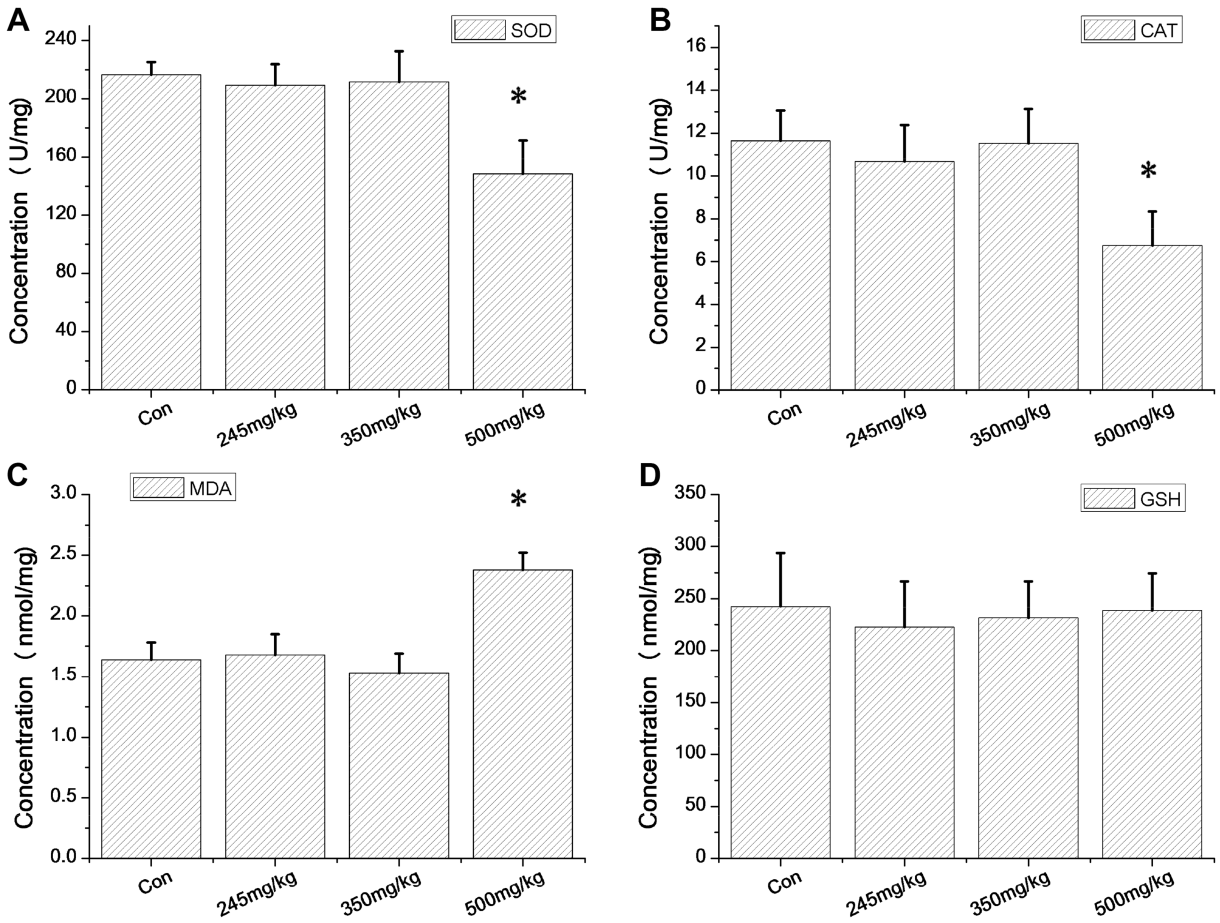

Figure 7 Oxidative stress indexes in the liver of ICR mice following single injection of ZrO_2. Mean and standard deviation of SOD, CAT, MDA and GSH of ICR mice (n=5 per group). The SOD level of the 350 and 500 mg/kg groups decreased significantly ($p<0.05$) comparing with control. The CAT level of the 500 mg/kg groups decreased significantly ($p<0.05$) comparing with control. The MDA level of the 500 mg/kg groups increased significantly ($p<0.05$) comparing with control. (*denotes statistical significance for the comparison of control, *$p<0.05$).

size of ZrO_2 trapped mainly in the liver and spleen was virtually the same as in vitro. Compared with the control group, no obvious ultrastructure changes were observed in the liver and spleen when the animal received ZrO_2 by intravenous injection. These results indicated that ZrO_2 NPs were recognized and internalized by the resident macrophages in the liver and spleen.

Stability of ZrO_2 NPs in simulate fluid

Particle sizes and TEM images of ZrO2 NPs were measured after 30 days incubation in the different simulated fluids. Table S3 shows the almost same size results (165±10 nm) of ZrO_2 in these fluids after 30 days incubation by DLS. The TEM images of NPs were shown in Figure S6. Compared with the original particles, there was no obvious change found in these particles after incubation in the acid (SGF) and alkaline solutions (SIF). These results indicated the well stability ZrO_2 in the internal environment for a month which with agree with the previous reports about the anti-acid and anti-alkaline activity of ZrO_2 materials [9, 10].

Zr content analysis

For further investigation of distribution of ZrO_2, ICP-OES analysis was used to reveal the changes of Zr contents varied from tissue to tissue. Figure 10 shows that the highest Zr levels were detected in the liver than other organs. And the Zr levels in liver and spleen peaked at 24 hrs and then declined over 4 weeks. Other tissues also experienced increased Zr contents 24 hrs after the ZrO_2 injection, but this increase was relatively smaller in heart, lung and kidney than liver and spleen tissues. The ICP-OES result is consistent with the histomorphology and TEM results. The gradual degradation of Zr levels in multi organs suggests ZrO_2 could be excreted from the body and the entire clearance of the particles required longer than 4 weeks.

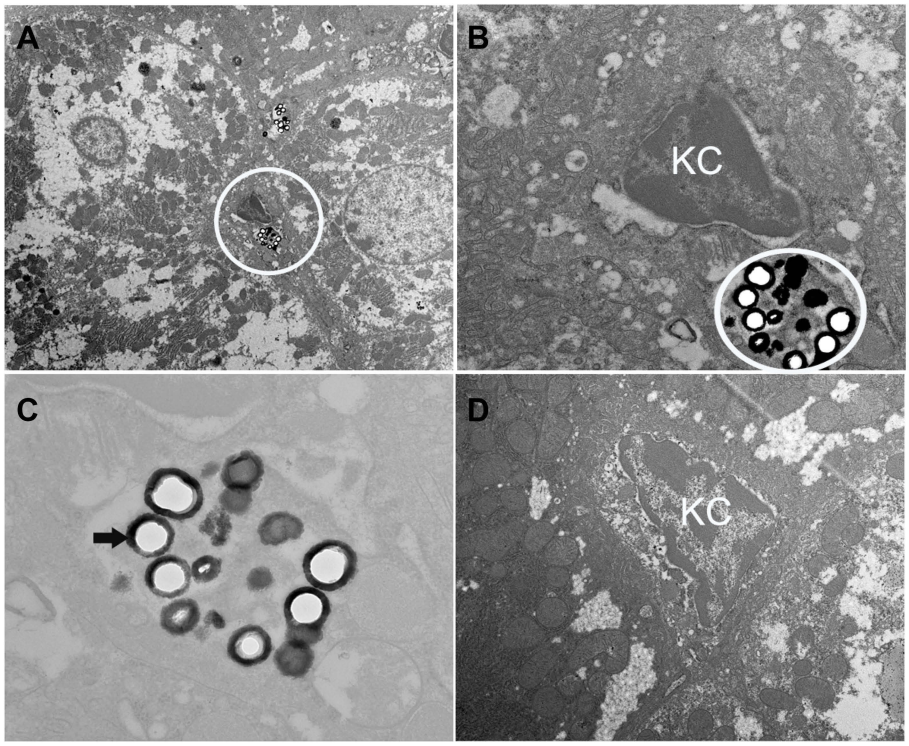

Figure 8 TEM images of treated mice liver (**A** ×6k, **B** ×15k and **C** ×30k) and control group (**D** ×15k) sacrificed 24 hrs post-injection with ZrO_2. Black arrow indicates ZrO_2 particles.
Abbreviation: KC, Kupffer cells.

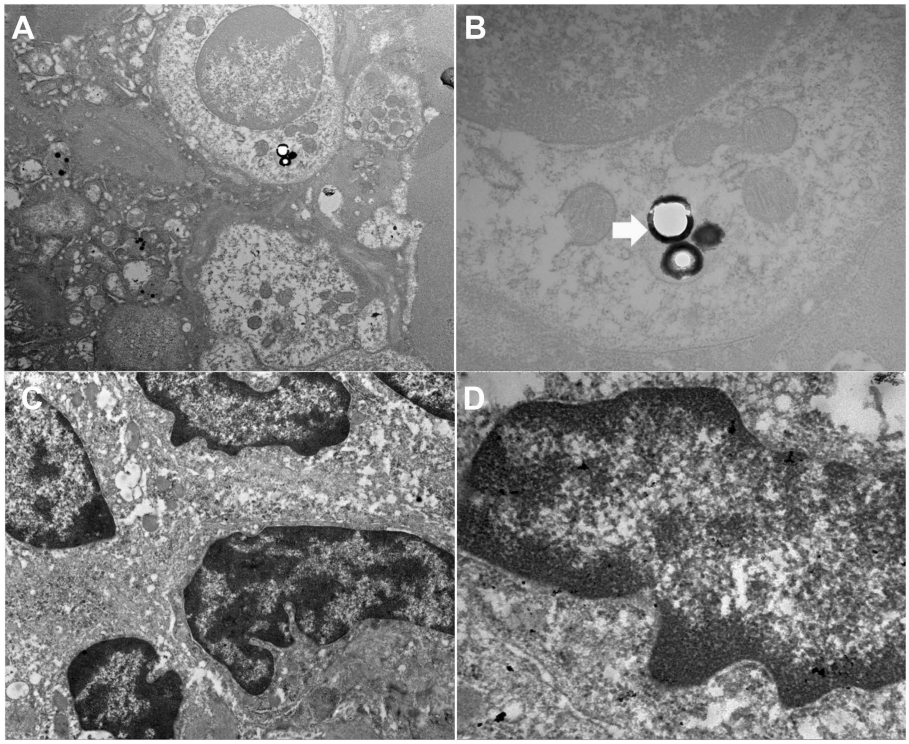

Figure 9 TEM images of treated mice spleen (**A**, ×6k and **B**, ×30k) and control group (**C**, ×15k and **D**, ×30k) sacrificed 24 hrs post-injection with ZrO_2. White arrow indicates ZrO_2 particles.

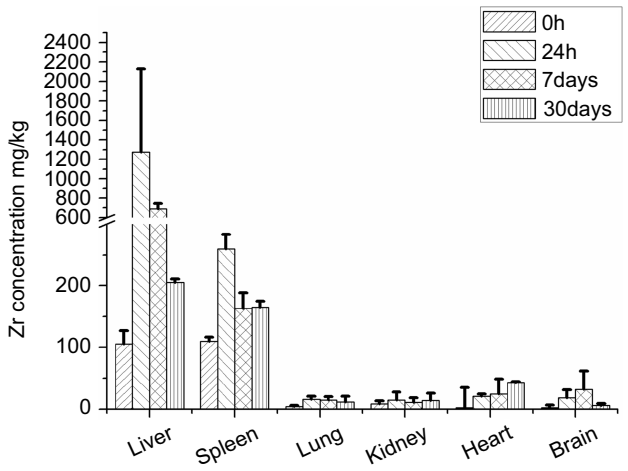

Figure 10 ICP-OES analysis result of Zr levels in liver, spleen, lung, kidney, heart and brain of animals treated with ZrO_2 (n=5 per group).

Conclusion

We investigated the acute toxicity and biodistribution of ZrO_2 after administered by intravenous in vivo. The results of weight, histomorphology, hematology and blood biochemical assay revealed a dose-dependent manner after single injection. The dosages of ZrO_2 in the range of 100–350 mg/kg are safe for clinical use. Although the results indicate involvement of oxidative damage in the liver and serum caused by ZrO_2 at high dose, more detailed information and molecular mechanisms are needed to confirm these results. Further evaluation of the excretion is needed, and the future studies based on these data will provide very useful information for development of drug delivery system using ZrO_2.

Ethics approval and consent to participate

Animal experimentation was governed by the Regulations of Experimental Animals of Beijing Authority. Animal Ethics Committee of the China Agriculture University approved the experiment.

Consent for publication

The authors confirm that the work described has not been published before and it is not under consideration for publication elsewhere. The publication has been approved by all co-authors.

Availability of data and material

All data generated or analyzed during this study are included in this published article and its supplementary information files.

Acknowledgments

The authors acknowledge the financial support from National Natural Science Foundation of China (project No. 61571426, 61671435, 31400854), National Hi-Tech. Research and Development Program of China (No. 2013AA032201), Beijing Natural Science Foundation (No. 4161003), and Young Teachers Innovation Project of China Agricultural University (2018QC142).

Author contributions

All authors contributed to data analysis, drafting and revising the article, gave final approval of the version to be published, and agree to be accountable for all aspects of the work.

Disclosure

The authors report no conflicts of interest in this work.

References

1. Nelson CA, Szczech JR, Xu Q, Lawrence MJ, Jin S, Ge Y. Mesoporous zirconium oxide nanomaterials effectively enrich phosphopeptides for mass spectrometry-based phosphoproteomics. *Chem Commun*. 2009;6607–6609. doi:10.1039/b908788e
2. Yu C, Liu G, Zuo B, Tang R. A novel gaseous dimethylamine sensor utilizing cataluminescence on zirconia nanoparticles. *Luminescence*. 2009;24:282–289. doi:10.1002/bio.1097
3. Soh M, Kang DW, Jeong HG, et al. Ceria-zirconia nanoparticles as an enhanced multi-antioxidant for sepsis treatment. *Angewandte Chemie*. 2017;56:11399–11403. doi:10.1002/anie.201704904
4. Figueroa-Lara JJ, Torres-Rodriguez M, Gutierrez-Arzaluz M, Romero-Romo M. Effect of zirconia nanoparticles in epoxy-silica hybrid adhesives to join aluminum substrates. *Materials*. 2017;10:10.
5. Larmier K, Liao WC, Tada S, et al. CO2 -to-methanol hydrogenation on zirconia-supported copper nanoparticles: reaction intermediates and the role of the metal-support interface. *Angewandte Chemie*. 2017;56:2318–2323. doi:10.1002/anie.201610166
6. Zare M, Ramezani Z, Rahbar N. Development of zirconia nanoparticles-decorated calcium alginate hydrogel fibers for extraction of organophosphorous pesticides from water and juice samples: facile synthesis and application with elimination of matrix effects. *J Chromatogr A*. 2016;1473:28–37. doi:10.1016/j.chroma.2016.10.071
7. Schunck A, Kronz A, Fischer C, Buchhorn GH. Release of zirconia nanoparticles at the metal stem-bone cement interface in implant loosening of total hip replacements. *Acta Biomater*. 2016;31:412–424. doi:10.1016/j.actbio.2015.11.044
8. Lohbauer U, Wagner A, Belli R, et al. Zirconia nanoparticles prepared by laser vaporization as fillers for dental adhesives. *Acta Biomater*. 2010;6:4539–4546. doi:10.1016/j.actbio.2010.07.002
9. Aivazi M, Hossein Fathi M, Nejatidanesh F, et al. The evaluation of prepared microgroove pattern by femtosecond laser on alumina-zirconia nano-composite for endosseous dental implant application. *Lasers Med Sci*. 2016;31:1837–1843. doi:10.1007/s10103-016-2059-8
10. Sun T, Guo M, Cheng Y, et al. Graded nano glass-zirconia material for dental applications-part II biocompatibility evaluation. *J Biomed Nanotechnol*. 2017;13:1682–1693. doi:10.1166/jbn.2017.2379

11. Sun T, Liu R, Liu X, Feng X, Zhang Y, Lai R. The biocompatibility of dental graded nano-glass-zirconia material after aging. *Nanoscale Res Lett*. 2018;13:61. doi:10.1186/s11671-018-2479-4
12. Kurtz SM, Kocagoz S, Arnholt C, Huet R, Ueno M, Walter WL. Advances in zirconia toughened alumina biomaterials for total joint replacement. *J Mech Behav Biomed Mater*. 2014;31:107–116. doi:10.1016/j.jmbbm.2013.03.022
13. Shi H, Niu M, Tan L, et al. A smart all-in-one theranostic platform for CT imaging guided tumor microwave thermotherapy based on IL@ZrO2 nanoparticles. *Chem Sci*. 2015;5016–5026. doi:10.1039/C5SC00781J
14. Koutayas SO, Vagkopoulou T, Pelekanos S, Koidis P, Strub JR. Zirconia in dentistry: part 2. Evidence-based clinical breakthrough. *Eur J Esthet Dent*. 2009;4:348–380.
15. Lughi V, Sergo V. Low temperature degradation -aging- of zirconia: a critical review of the relevant aspects in dentistry. *Dent Mater*. 2010;26:807–820. doi:10.1016/j.dental.2010.04.006
16. Fathima JB, Pugazhendhi A, Venis R. Synthesis and characterization of ZrO2 nanoparticles-antimicrobial activity and their prospective role in dental care. *Microb Pathog*. 2017;110:245–251. doi:10.1016/j.micpath.2017.06.039
17. Quan R, Tang Y, Huang Z, Xu J, Wu X, Yang D. Study on the genotoxicity of HA/ZrO2 composite particles in vitro. *Mater Sci Eng C Mater Biol Appl*. 2013;33:1332–1338. doi:10.1016/j.msec.2012.12.033
18. Otero-Gonzalez L, Garcia-Saucedo C, Field JA, Sierra-Alvarez R. Toxicity of TiO(2), ZrO(2), Fe(0), Fe(2)O(3), and Mn(2)O(3) nanoparticles to the yeast, Saccharomyces cerevisiae. *Chemosphere*. 2013;93:1201–1206. doi:10.1016/j.chemosphere.2013.06.075
19. Oyanagui Y. Reevaluation of assay methods and establishment of kit for superoxide dismutase activity. *Anal Biochem*. 1984;142:290–296.
20. Aebi H. Catalase in vitro. *Methods Enzymol*. 1984;105:121–126.
21. Ohkawa H, Ohishi N, Yagi K. Assay for lipid peroxides in animal tissues by thiobarbituric acid reaction. *Anal Biochem*. 1979;95:351–358.
22. Weidemann G. [Interference by glutathione reductase in the GSH-activated determinated of creatine kinase in serum (author's transl)]. *Z Klin Chem Klin Biochem*. 1973;11:134–135.